# WEAK LENSING BY INDIVIDUAL GALAXIES

TEREASA G. BRAINERD
*Department of Astronomy, Boston University*
*725 Commonwealth Ave., Boston, MA 02215*

ROGER D. BLANDFORD
*California Institute of Technology*
*Theoretical Astrophysics 130-33, Pasadena, CA 91125*

AND

IAN SMAIL
*Observatories of the Carnegie Institution of Washington*
*813 Santa Barbara St., Pasadena, CA 91101*

## 1. Introduction

In this paper we report on an investigation of statistical weak gravitational lensing of cosmologically distant faint galaxies by foreground galaxies. The signal we seek is a distortion of the images of faint galaxies resulting in a weakly preferred tangential alignment of faint galaxies around brighter galaxies. That is, if the faint galaxies have been gravitationally lensed by the brighter systems, the major axes of their images will tend to lie perpendicular to the radius vectors joining the centroids of the faint and bright galaxies (Fig. 1). Modeling a lens galaxy as a singular isothermal sphere with circular velocity $V_c$, an ellipticity of $\sim 2\pi V_c^2/c^2\theta$ is induced in the image of a source galaxy at an angular separation $\theta$ from the lens. This is of order a few percent for faint–bright galaxy pairs with separations $\theta \sim 30''$ where the lens is a typical bright spiral. Over 1000 pairs must be measured in order to detect such a signal in the presence of the noise associated with the intrinsic galaxy shapes. Given a sufficiently large number of pairs, it may be possible to use the variation of the induced ellipticity with $\theta$ to study the angular extent of the halos of the lens galaxies.

Tyson et al. (1984) investigated such galaxy–galaxy lensing using scans of photographic plates (cf. also Webster (1983)) from which they obtained
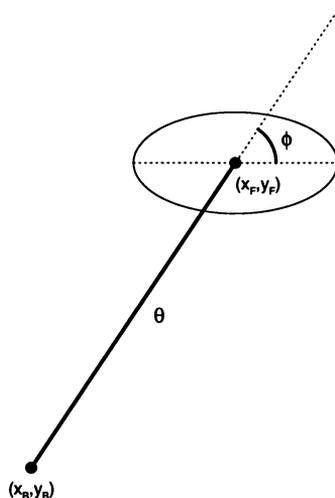
*Figure 1.*   Orientation of faint galaxies relative to bright galaxies.

images of $\sim 47,000$ faint galaxies ($22.5 < J < 23.5$) and $\sim 12,000$ bright galaxies ($19 < J < 21.5$). For faint–bright galaxy separations greater than $\sim 3''$, no statistically significant deviation from an isotropic distribution of faint image orientations was found.

## 2.  Observational Data

The imaging data used for our analysis is expected to be of sufficient quality, depth, and size to allow a detection of galaxy–galaxy lensing. The data are of a single $9.6' \times 9.6'$ blank field centered on $\alpha(1950) = 17^h 21^m 07^s$ $\delta(1950) = +49°52'21''$, taken in Gunn $r$, and were acquired during periods of good seeing ($0.7''$–$0.9''$) using the COSMIC imaging spectrograph (Dressler et al. 1995) on the 5-m Hale telescope. The reduction of the data to a catalogue of detected objects is detailed in Mould et al. (1994).

The final stacked frame consists of a total of 19 individual frames with a cumulative exposure time of 24.0 ksec. The final frame has a $1\sigma$ surface brightness limit of $\mu_r = 28.8$ mag arcsec$^{-2}$, seeing of $0.87''$ FWHM, and total area of 90.1 arcmin$^{-2}$. Due to the presence of classical distortion in the corners of the frame, all analysis is restricted to those objects which lie within a circle of radius $4.8'$, centered on the chip. There are 4819 galaxies in this area brighter than the $\sim 97\%$ completeness limit of $r = 26.0$.

The probability distribution of the image ellipticities in the sample (which, to linear order, is equivalent to the distribution of the intrinsic source galaxy ellipticities) is adequately fit by $P_\epsilon(\epsilon) = 64\epsilon \exp[-8\epsilon]$ with mean ellipticity $\langle \epsilon \rangle = 0.25 \pm 0.02$.
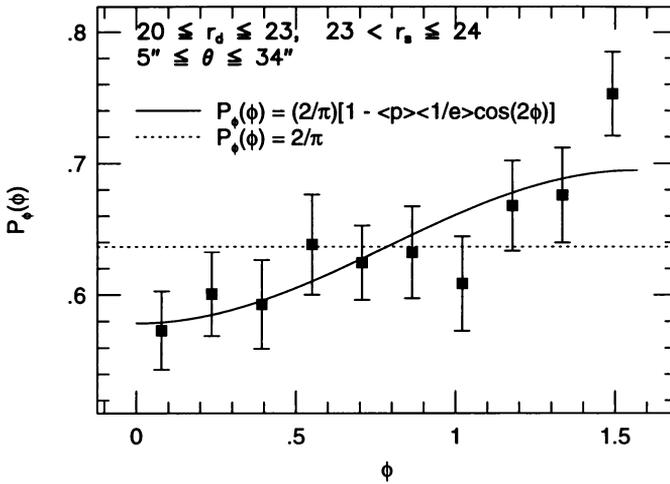
*Figure 2.* Probability distribution of faint image orientation relative to bright galaxies.

## 2.1. POSITION ANGLE PROBABILITY DISTRIBUTION

We have investigated the probability distribution, $P_\phi(\phi)$, of the orientations of the resolved images of faint galaxies ($23 < r_s \le 24$; 511 objects) relative to brighter galaxies ($20 \le r_d \le 23$; 439 objects) as in Fig. 1. Since we are primarily interested in distinguishing between radial and tangential alignments, positive and negative position angles of the faint galaxies were combined so that $\phi$ is restricted to the range $[0, \pi/2]$. In Fig. 2, $P_\phi(\phi)$ evaluated using annuli with $5'' \le \theta \le 34''$, centered on the bright galaxies, is shown. Error bars were obtained by bootstrap resampling. The inner annulus radius avoids overlapping faint–bright image isophotes and the outer radius should roughly maximize the signal to noise for our data set. With this annulus we obtain 3202 faint–bright pairs and, thus, each faint galaxy is paired with a number of near neighbor bright galaxies. In the case of galaxy–galaxy lensing $\sim 2/3$ of the sources will have encountered 2 or more significant deflectors and, therefore, to optimize the ability to detect the lensing signal it is necessary to average the faint image orientation over all possible deflectors.

Under the assumptions of random intrinsic faint galaxy orientations and no gravitational lensing by the brighter galaxies, $P_\phi(\phi)$ should be consistent with a uniform distribution ($P_\phi(\phi) = 2/\pi$). A $\chi^2$ test performed on the binned distribution $P_\phi(\phi)$ in Fig. 2 rejects a uniform distribution at a confidence level of 97.9%, while a Kolmogorov-Smirnov test performed on the continuous, cumulative distribution of $P_\phi(\phi)$ rejects a uniform distribution at a confidence level of 99.9%. In the case of gravitational lensing $P_\phi(\phi)$

should exhibit a $\cos 2\phi$ variation of the form $P_\phi(\phi) = \frac{2}{\pi}[1 - \langle p \rangle \cos 2\phi \langle \epsilon^{-1} \rangle]$, where $\langle p \rangle$ is the mean image polarization. From the image ellipticity distribution $\langle \epsilon^{-1} \rangle = 8.0$. Shown in Fig. 2 is the best-fit $\cos 2\phi$ variation of this form, from which we infer $\langle p \rangle = 0.011 \pm 0.006$ (95% confidence bounds).

A number of null tests were performed to investigate possible systematic effects in the data which would give rise to the observed non-uniform $P_\phi(\phi)$. The tests include (i) $\phi$ as the orientation of the bright galaxies relative to the faint galaxies, (ii) $\phi$ as the orientation of the faint galaxies relative to random points, (iii) $\phi$ as the orientation of the faint galaxies relative to stars, and (iv) a random $\phi$ was substituted for the true faint image $\phi$. In all cases $P_\phi(\phi)$ is consistent with a uniform distribution.

The image polarization of the faint galaxies is robust to splitting of the data into subsamples. Considering (i) positive values of $\phi$ independently of negative values of $\phi$, (ii) objects within $3.4'$ of the center of the chip vs. objects farther than $3.4'$ from the center of the chip, and (iii) objects within each of the north, south, east, and west $1/2$ circles of radius $4.8'$, $P_\phi(\phi)$ is inconsistent with a uniform distribution and $\langle p \rangle$ obtained for the subsamples is consistent with that obtained using the full sample.

From determinations of $P_\phi(\phi)$ for the faint galaxies using independent bins, $\theta$, the variation of $\langle p \rangle$ with lens–source separation was computed. Results are shown in Fig. 3, where the error bars are the formal $1\sigma$ error from the least squares fit of the $\cos 2\phi$ variation to $P_\phi(\phi)$.

## 3. Implications of Image Polarization for Lens Halos

From the variation of $\langle p \rangle$ with $\theta$ (Fig. 3), measured properties of local galaxies, and modest extrapolations of the observed redshift distribution of faint galaxies, formal best–fit parameters for the dark halos of the lens galaxies can be derived. Modeling the mass distribution of the halos as

$$\rho(r) = \frac{V_c^2 s^2}{4\pi G r^2 (r^2 + s^2)}, \tag{1}$$

where $V_c$ is the de-projected circular velocity for $r \ll s$ and $s$ is an outer scale radius beyond which $\rho(r) \propto r^{-4}$, we find the image polarization is

$$p(X) = \frac{2\pi V_c^2 D_d D_{ds}}{s D_s c^2} \frac{(2 + X)(1 + X^2)^{1/2} - (2 + X^2)}{X^2(1 + X^2)^{1/2}}, \tag{2}$$

where $D_d$, $D_s$, $D_{ds}$ are angular diameter distances and $X$ is the ratio of the projected lens–source separation and $s$.

We introduce two characteristic scaling parameters, $V^*$ and $s^*$, by assuming that the circular velocity scales as the fourth root of the total luminosity in a given band (in agreement with the Tully-Fisher relation) and
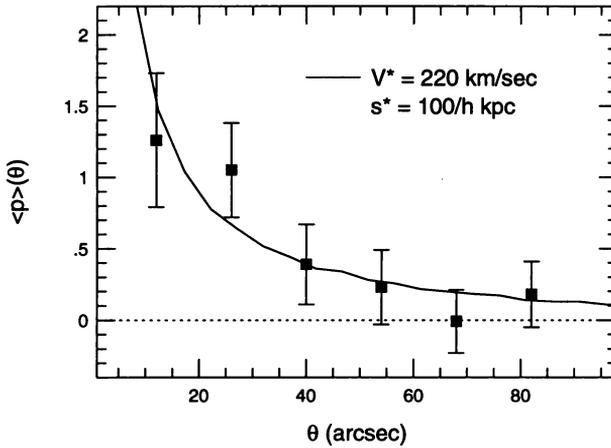
*Figure 3.* Observed variation of faint image polarization with differential lens–source (points with error bars) and model prediction (solid line).

that the total mass-to-light ratio of a galaxy is a constant independent of its luminosity, obtaining

$$\frac{V_c}{V^*} = \left(\frac{L_\nu}{L_\nu^*}\right)_r^{1/4} \qquad \frac{s}{s^*} = \left(\frac{L_\nu}{L_\nu^*}\right)_r^{1/2} = \left(\frac{M}{M^*}\right)^{1/2}, \qquad (3)$$

where $L^*$ and $M^*$ are the characteristic luminosity and mass, respectively. Allowing for a spectral (or "K") correction we have

$$\frac{L_\nu}{L_\nu^*} = \left(\frac{H_0 D_d}{c}\right)^2 (1+z)^{3+\alpha} 10^{0.4(23.9-r)}, \qquad (4)$$

where $\alpha \equiv -d\ln L_\nu/d\ln\nu \sim 3$, very approximately. We use a parameterized redshift distribution of the form

$$F(z,r) = \frac{\beta z^2 e^{-(z/z_0)^\beta}}{\Gamma(3/\beta)z_0^3} \qquad (5)$$

and for our fiducial model we adopt $\beta = 1.5$. More generally for $20 < r < 24$, $z_0 = k_z[z_m + z_m'(r-22)]$, where $k_z = 0.7$ for $\beta = 1.5$, and $z_m' = 0.1$ fiducially. For $20 \le r \le 23$ the parameterized redshift distribution is in good agreement with observation (eg. Lilly 1993; Tresse et al. 1993) and for simplicity we assume that the general form can be extended to $r = 24$.

Using the above relations Monte Carlo simulations of galaxy–galaxy lensing were carried out for sets of parameters $(V^*, s^*)$ for galaxies with magnitudes in the range $20 \le r \le 24$. For each source galaxy the net

polarization due to all deflectors was determined and the variation of $\langle p \rangle$ with $\theta$ for the $23 < r \leq 24$ Monte Carlo galaxies computed and compared to the observed $\langle p \rangle (\theta)$ using a $\chi^2$ test. The values of $V^*$ and $s^*$ were varied until $\chi^2$ reached a minimum, resulting in formal best-fit values for the characteristic halo parameters. An Einstein-DeSitter universe was adopted; however, the results obtained are relatively insensitive to the cosmogony.

From the $\chi^2$ minimization the best-fit characteristic halo parameters are $V^* = 220 \pm 80$ km sec$^{-1}$ (90% confidence bounds) and $s^* \gtrsim 100 h^{-1}$ kpc, for which the $\chi^2$ per degree of freedom is of order 0.6. The image polarization is relatively insensitive to the outer scale parameter $s^*$ and, since most of the signal is contributed by lenses that are sufficiently close to the source on the sky that the line of sight passes through the isothermal part of the halo and for large halos the average polarization is approximately independent of $s$, it is not possible to obtain a unique best-fit value of $s^*$.

From our limits on the best-fit $V^*$ and $s^*$ we estimate the characteristic masses of the lens halos within a radius $r$ to be $M(100 h^{-1}\text{kpc}) \sim 1.0^{+1.1}_{-0.7} \times 10^{12} h^{-1} M_\odot$ and $M(150 h^{-1}\text{kpc}) \sim 1.4^{+1.8}_{-1.0} \times 10^{12} h^{-1} M_\odot$, consistent with the dynamical estimates of the masses of field spirals by Zaritsky & White (1994) for which they obtain $M(150 h^{-1}\text{kpc}) \sim 1-2 \times 10^{12} h^{-1} M_\odot$. Although our result is somewhat sensitive to the model parameters adopted, the consistency with the dynamical mass estimate is encouraging since the two methods rely on completely different sets of underlying assumptions.

## References

Dressler, A., et al., 1995, in preparation
Lilly, S., 1993, ApJ, 411, 501
Mould, J., Blandford, R., Villumsen, J., Brainerd, T., Smail, I., Small, T., & Kells, W., 1994, MNRAS, 271, 31
Tresse, L., Hammer, F., LeFevre, O., & Proust, D., 1993, A&A, 277, 53
Tyson, J.A., Valdes, F., Jarvis, J.F., & Mills, A.P., 1984, ApJL, 281, L59
Webster, R.L., 1983, PhD Thesis, University of Cambridge
Zaritsky, D. & White, S.D.M., 1994, ApJ, 435, 599